DOI: 10.1002/ejoc.201101351

Hydrogen-Bond-Assisted Helical Folding of Propeller-Shaped Molecules: Effects of Extended π-Conjugation on Chiral Selection, Conformational Stability, and Exciton Coupling

Elizabeth A. Opsitnick,[a] Xuan Jiang,[a] Andrew N. Hollenbeck,[a] and Dongwhan Lee*[a]

Keywords: Helical structures / Conformation analysis / Chiral induction / Hydrogen bonds / Exciton coupling

Cooperative interaction between multiple chiral centers dictates the absolute handedness of structural folding. We have designed and prepared a series of chiral C_3-symmetric tris(*N*-salicylidenamine) derivatives that adopt three-blade propeller-like conformations. Synthetic access to an expanded family of such constructs was aided by enzymatic resolution and C–C cross-coupling reactions of aryl-substituted chiral propargylic alcohol derivatives. These key structural components were integrated into molecular propellers of predetermined helical screw sense. Through comparative studies on a homologous set of molecules, we found that installation of phenylene-ethynylene-derived π-conjugation profoundly affected the stabilities of the helically folded structures, as evidenced by UV/Vis and circular dichroism (CD) studies. Increasing the number of hydrogen bonds through additional substitution also enhanced the populations of the folded conformations in solution. In addition to introducing steric bias to control structural folding, linearly π-conjugated groups function as spatially well-defined chromophores that give rise to characteristic exciton-coupled circular dichroism. Absolute configurations of chiral centers could thus be further confirmed by comparing the torsional relationships between pairs of chromophores on adjacent subunits, which are fully consistent with the computationally predicted structural models.

Introduction

Spontaneous folding of well-designed linear molecules gives rise to compact secondary structures that are stabilized by multiple noncovalent bonds.[1–3] As is exemplified by naturally occurring macromolecules such as proteins, polynucleic acids, and polysaccharides, restriction of bond rotations around the molecular backbones of such constructs often helps simplify the reaction coordinates of the structural folding process. In addition, the intricate side chain–side chain and/or backbone–side chain interactions provide energetic bias toward the desired conformation against potentially competing species.[4] Particularly useful in this context is the concept of *negative design*,[5] in which energy-destabilizing structural motifs are intentionally introduced in order to increase the penalty of "misfolding" and thereby to define a steeper energy landscape that will quickly converge to the correctly folded structure. This design principle has frequently been applied to the de novo construction of proteins[6] and their synthetic mimetics.[1–3]

Foldamers represent an emerging class of synthetic molecules that are designed to fold into well-defined three-dimensional (3D) structures.[1–3] Here, strategic placement of multiple noncovalent interactions between non-neighboring positions along the rigid backbone helps guide the formation of robust secondary structures in solution. Existing paradigms in such endeavors focus predominantly on the formation of helical objects that present functional groups on the convex or concave side of the cavity to assist self-association,[7] guest recognition,[1q,7h,7g,8–13] or catalysis.[14]

As shown in Scheme 1, spiral folding of a linear foldamer **A** could proceed in either a right- or a left-handed manner to furnish helical objects of opposite handedness (i.e., *P* or *M* conformations). Positioning of chiral auxiliaries, typically in the form of pendant aliphatic chains[7e,13d,13f,15–18] or twisted arene–arene backbone skeletons,[19] can potentially bias this process toward one screw sense over the other.

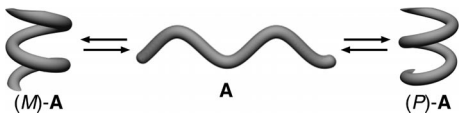

Scheme 1. Structural folding of a linear foldamer **A** to adopt either a right-handed *P* conformation or a left-handed *M* conformation.

We have recently shown that intuitive chiral induction models developed for linear foldamers can readily be adapted for dendritic structures that spontaneously fold to adopt propeller-shaped geometries.[20] As shown in Scheme 2, close steric contacts between the three mobile components ("blades") constituting the stereodynamic

[a] Department of Chemistry, Indiana University
800 East Kirkwood Avenue, Bloomington, Indiana 47405, USA
Fax: +1-812-855-8300
E-mail: dongwhan@indiana.edu

Supporting information for this article is available on the WWW under http://dx.doi.org/10.1002/ejoc.201101351.

structure **B** dictate that their tilting motions proceed in a unidirectional fashion to provide either a right-handed *P* conformer or a left-handed *M* conformer.[21,22] Classical examples of such stereodynamic systems include C_3-symmetric triarylcarbonium and triarylcyclopropenium cations, in which torsional motions occurring at different parts of the molecule are correlated through tight van der Waals contacts.[23] In inorganic systems with threefold symmetry, similar structural interconversions between the *P* and *M* isomers occur through concerted tilting motions of bulky ligands.[24]

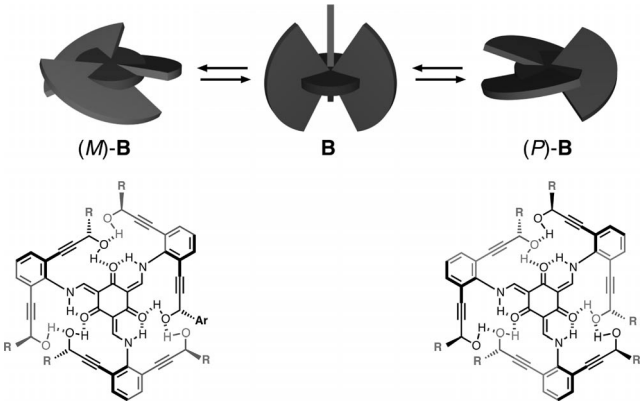

Scheme 2. Stereochemical interconversion of the propeller-shaped molecule **B** between a right-handed *P* conformer and a left-handed *M* conformer. Structural folding proceeds through concerted tilting motions of three "blades", which correspond to the three aryl groups that are attached directly to the C_3-symmetric molecular core of tris(*N*-salicylidenamine) shown below the schematic diagram. For achiral tris(*N*-salicylidenamine)s with R = H, the *M* and *P* conformations are enantiomers and isoenergetic. For chiral tris(*N*-salicylidenamine)s with R ≠ H, the *M* and *P* conformations are not mirror images of one another but are diastereomeric, and therefore differ in energy.

We postulated that the introduction of steric bias at such *intersubunit* contacts should dictate the absolute screw sense, either *P* or *M*, of structural folding, and that this process could be assisted by the principles of *negative design*.[5] Our first-generation molecular prototypes – $(S,S)_3$-**2** (Figure 1) and its mirror-image isomer $(R,R)_3$-**2** – were thus constructed with the use of tris(*N*-salicylidenamine)[20,25–27] as the C_3-symmetric core and three 2,6-disubstituted aryl groups as the blades. Through the installation of bulky phenyl groups as part of the chiral secondary alcohol groups at the "wingtips", we wished to enhance repulsive van der Waals interactions in the *misfolded* conformations so that the correctly folded structure would be further stabilized in the relative energy scale. As shown in Figure 1, in the choice between the right-handed and the left-handed structure, $(S,S)_3$-**2** preferentially adopts the *M* conformation, in which phenyl groups point *away from* the center of the molecule in order to avoid undesired steric congestion. The mirror-image relationship dictates that its enantiomer $(R,R)_3$-**2** should prefer the right-handed *P* conformation, which was also confirmed experimentally.

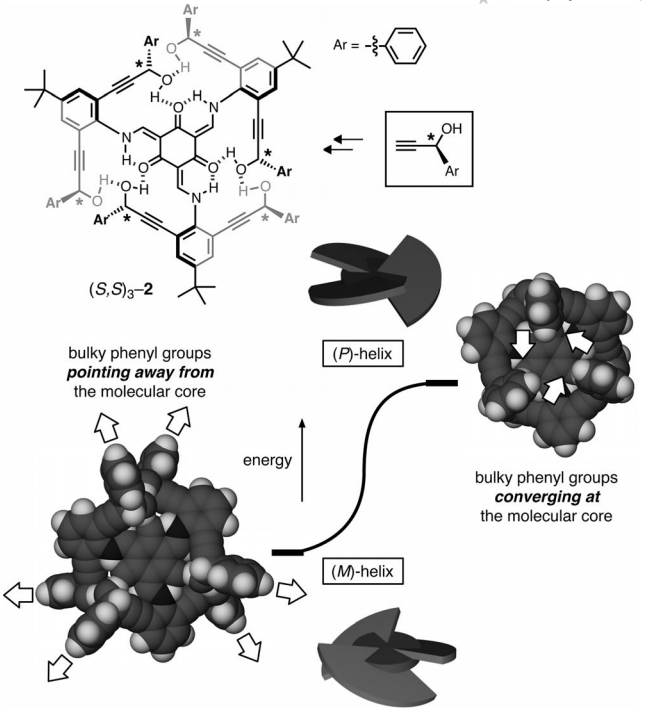

Figure 1. Chemical structure of $(S,S)_3$-**2** and space-filling models of *M* and *P* helical conformations obtained by hydrogen-bonding-assisted structural folding.[20] The "misfolded" *P* chiral conformation suffers from steric congestion between phenyl groups that converge at the molecular core. As a consequence, it is energetically destabilized with respect to the *M* conformer, which is the "correctly folded" form of the molecule (NOTE: these conformers are not mirror images of one another but are diastereomeric and therefore differ in energy).

This stereoinduction model immediately established a direct correlation between the absolute configuration (either *R* or *S*) of the chiral centers at the dendritic termini and the preferred screw sense (either *P* or *M*) of the folded molecule. DFT single-point energy (SPE) calculations on model compounds and TD-DFT analysis of experimentally determined CD spectra fully supported the validity of our initial proposal of central-to-helical chirality transfer.[20]

In order to develop these stereoinduction models, to refine them further, and to obtain direct experimental evidence for assignation of absolute screw sense by exciton-coupled circular dichroism (ECCD),[28] we decided to explore an expanded family of chiral tris(*N*-salicylidenaniline) molecules. In addition to enhancing the stability of the preferred helical conformation in solution, extended π-conjugation installed at the wingtip chiral groups of these molecules enables them to function as spatially well-defined chromophores with low excitation energies. Notably, the ECCD spectral patterns arising from well-defined pairwise spatial relationships of these extended π-conjugated substituents are fully consistent with computational models and further support the validity of our chiral induction model. A systematic analysis on the effects of i) the sizes of the chiral substituents, ii) the number of hydrogen bonds, and iii) solvent environments on the structural folding of these new chiral tris(*N*-salicylidenamine)s constitutes the main

topic of this contribution. As in the de novo design of proteins,[5b] destabilization of an undesired interaction becomes as important as stabilization of a desired interaction in our synthetic systems, the details of which are provided in the following sections.

Results and Discussion

Design Principles – "Negative Design" in the Promotion of Chiral Bias

The DFT energy-minimized structure of $(S,S)_3$-**2** served as the logical starting point in our structural reengineering directed towards systematic modulation of the conformational stability and chiral bias. As shown in Figure 1, the preference of $(S,S)_3$-**2** for the *M* conformation originates from the unfavorable steric interactions between the phenyl groups in the competing *P* conformation, which account for an 8.7 kcal mol^{-1} energy difference as estimated by PM3-level calculations.[29] In the disfavored *P* conformation, the phenyl rings on the wingtip alcohol groups point *toward* the center of the molecule (Figure 1). We thus reasoned that either linear extension at the *para*-position or substitution on the 3- and 5-positions should enhance sterically unfavorable contacts between the wingtip groups. It was anticipated that the increasing energy penalty of overcrowding in such π-extended groups should enhance the bias toward the *M* over the *P* conformer further, which is evident from comparison of the geometry-optimized models of $(S,S)_3$-**2** (Figure 1) and $(S,S)_3$-**4** (see Figures 2 and 3). Consistently with our intuitive prediction, the energy difference between the *P* and *M* conformers, calculated at the PM3 level, increases significantly from 8.7 kcal mol^{-1} for $(S,S)_3$-**2** to 17.8 kcal mol^{-1} for $(S,S)_3$-**4** (Table S1 in the Supporting Information).[29]

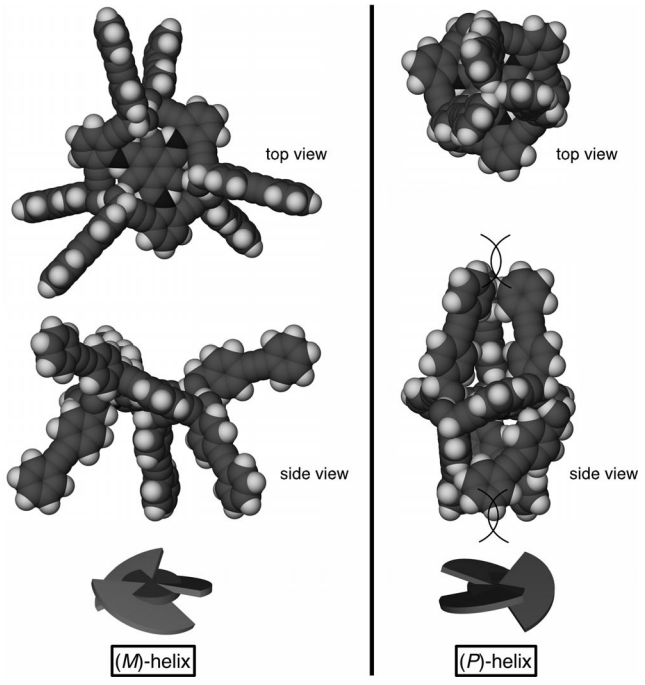

Figure 2. Space-filling models of PM3 geometry-optimized structures of $(S,S)_3$-**4** and cartoon-type renditions to describe the propeller-like arrangements of three aniline rings which are unidirectionally tilted either in left-handed fashion (for the *M* helix) or in right-handed fashion (for the *P* helix) (NOTE: these conformers are not mirror images of one another but are diastereomeric, and therefore differ in energy). In the case of the *M* helix (left), the six (phenylethynyl)phenyl groups on the wingtip alcohol groups all point away from the molecular core. Upon reversal of the helical screw sense, however, these groups converge to create highly congested steric environments both above and below the core plane of the *P* helix shown on the right. The *tert*-butyl groups on the *para*-positions of the aniline rings are removed for clarity in this drawing.

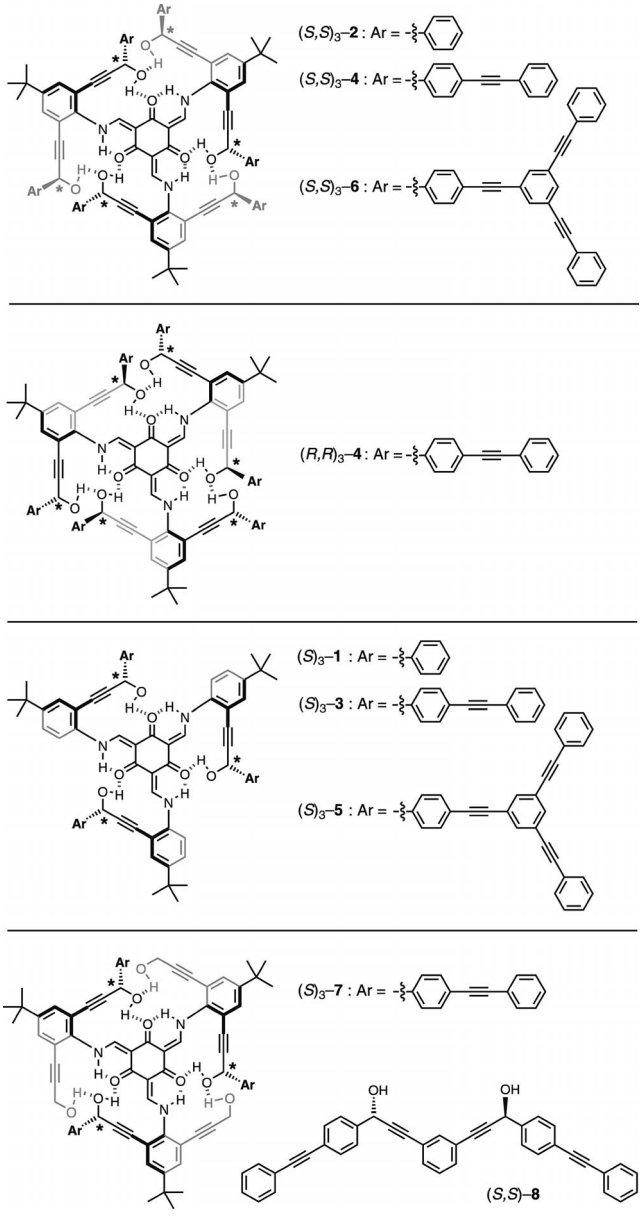

Figure 3. Chemical structures of the chiral tris(*N*-salicylideneamine)s **1**–**7** and of the subunit model compound **8**. The symbol $(S)_3$- here denotes the presence of three *S* chiral alcohol groups in the molecule; $(S,S)_3$- for six such groups. Note that $(R,R)_3$-**4** is the enantiomer of $(S,S)_3$-**4** (shown in Figure 2), and therefore has six *R* chiral alcohol groups.

A series of chiral tris(*N*-salicylidenamine) derivatives – compounds **3**–**7** (Figure 3) – and the chiral subunit model **8** were thus identified as logical synthetic targets in which variations were made in i) the number, ii) the absolute configuration, and iii) the steric bulk of the substituents on the wingtip chiral alcohol groups engaged in intramolecular hydrogen bonds. We anticipated that comparative spectroscopic studies on these new molecules and on the previously reported **1** and **2**[20] (see Figures 1 and 3) should help in the construction of more comprehensive structure–property models for chiral induction and conformational stability.

Chiral Alcohols as Key Synthetic Intermediates

Optically active secondary propargylic alcohols are useful synthons for chemical synthesis.[30] Typical strategies to access these chiral building blocks include i) asymmetric addition of acetylides to aldehydes or ketones,[30d,31] ii) asymmetric reductions of ketones,[32] and iii) enzymatic resolution of racemic alcohols.[33]

Asymmetric additions of terminal acetylides to a series of alkyl or aryl aldehydes with the aid of a catalytic system consisting of zinc triflate and optically active *N*-methylephedrine provide high yields and high enantioselectivities.[30d,31e,34] Although this method has shown that enantioselectivities are high for aromatic aldehydes (94–96%), the yields are considerably lower (ca. 50%) than in the case of aliphatic aldehydes (>90%).[34a] For the preparation of large quantities of chiral building blocks for our chemistry, enzymatic resolution of racemic alcohols thus became an appealing method. The reactions could be carried out under standard benchtop conditions without the requirement for strictly anhydrous reaction media. In addition, the resin-bound enzyme could be recovered and recycled without significant diminution of its reactivity and selectivity. One of the most attractive aspects of this method is that both *R* and *S* enantiomers could be accessed with use of one enzyme (vide infra), rather than by use of two different, and costly, catalysts for each enantiomer, as would be necessary with asymmetric addition or reduction protocols.

A lipase isolated from *Candida antarctica*, known commercially as Novozyme 435, is an effective catalyst in the resolution of aryl propargylic alcohols.[33] With this enzyme and vinyl acetate, the *R* alcohol is selectively esterified to leave the *S* alcohol behind (Scheme 3).

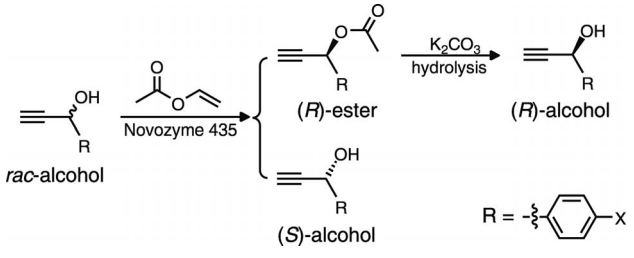

Scheme 3. Enzymatic resolution of aryl propargylic alcohols. The assignment of the absolute configuration here is based on R = 4-X-C_6H_5.

This enzymatic protocol has proven to be selective for the resolution of racemic aryl alcohols.[33b,33d,33f] Several different *para*-substituents on the phenyl group, including F and Cl, had previously been screened in kinetic resolutions of propargylic alcohols with the aid of Novozyme 435.[33d] In each case, the *R* alcohol was selectively esterified to leave behind the *S* alcohol with good yield (30–47%; max theoretical yield = 50%) and enantioselectivity (>98%). Encouraged by these precedents, we reasoned that a *para*-iodo substituent on the phenyl ring should not change the selectivity toward esterification of the *R* alcohol and decided to employ 4-iodobenzaldehyde and ethynylmagnesium bromide to prepare *rac*-**10** as the key intermediate in our synthesis (Scheme 4).

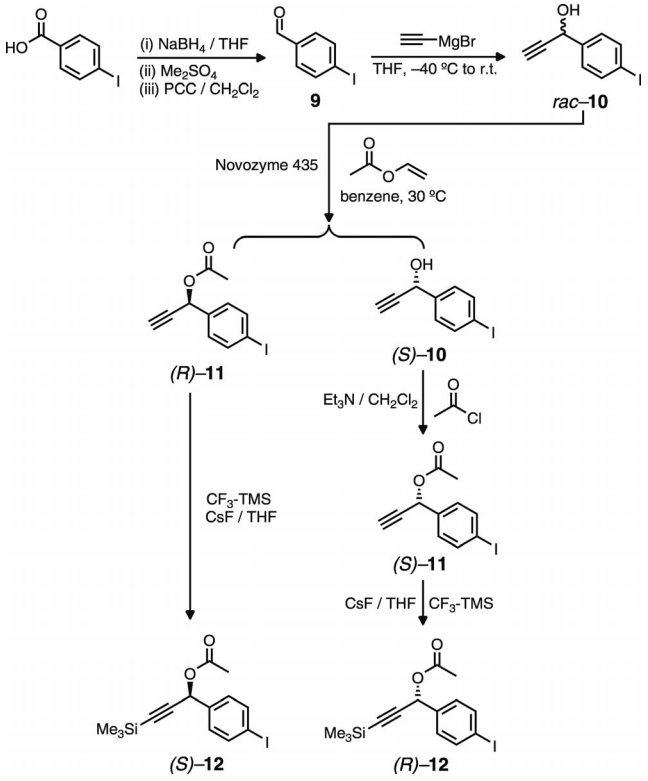

Scheme 4. Synthetic routes to the enantiomeric pair of protected propargylic alcohol derivatives (*S*)-**12** and (*R*)-**12**. Note the formal change in *R* vs. *S* assignment upon silylation of the ethynyl group of **11**.

After enzymatic resolution and subsequent functional group transformation, each enantiomer (i.e., *R* and *S*) could be elaborated further by standard cross-coupling reactions at the *para*-position to install ethynylenearyl moieties with different branching patterns. One of the most attractive features of this synthetic plan is its inherent modularity, through which a diverse array of π-extended chiral propargylic alcohols could be i) readily accessed from a common synthetic precursor, and ii) quickly integrated into the C_3-symmetric synthetic targets (Figure 3) through a finite number of synthetic operations.

Access to Chiral Building Blocks – Enzymatic Resolution and Extension of π-Conjugation

A one-pot reduction/oxidation of 4-iodobenzoic acid was carried out in quantitative yield to furnish **9** (Scheme 4).[35]

Addition of ethynylmagnesium bromide to **9** yielded *rac*-**10** in good yield (78%), and this compound was enzymatically resolved to afford the *R* ester **11** and the *S* alcohol **10**. We anticipated that the iodo substituent at the *para*-position of *rac*-**10** should have little effect on the enantioselective esterification of the *R* alcohol, as established for structurally related compounds.[33d] Enzymatic resolution with Novozyme 435 was thus carried out with *rac*-**10** under standard conditions (benzene, T = 30 °C) and the progress of the asymmetric esterification reaction with vinyl acetate was monitored by chiral HPLC. The purity of (*R*)-**10** was verified after isolation and subsequent hydrolysis of the ester (*R*)-**11**. The chiral HPLC chromatogram of (*R*)-**10** was compared to that of *rac*-**10** and found to represent >99% *ee* (Figure S2 in the Supporting Information). The purity of the unreacted (*S*)-**10**, after isolation by column chromatography, was also checked by chiral HPLC.[36] Although the purities of (*R*)-**10** and (*S*)-**10** were confirmed by chiral HPLC, it was necessary to verify the absolute configuration of each enantiomer. For this purpose, Mosher's ester method[37] was used to convert each alcohol into the corresponding (*R*)- and (*S*)-MTPA [α-methoxy-α-(trifluoromethyl)phenylacetic acid] esters. These compounds were analyzed by ^{1}H NMR spectroscopy (Table S2 in the Supporting Information) to establish fully the absolute stereochemistries depicted in Scheme 3 and Scheme 4.

For subsequent chemical transformations with C–C coupling, the ethynyl group of (*R*)-**11** needed to be protected in order to prevent self-coupling under Sonogashira–Hagihara reaction conditions. Typical protocols employing deprotonation with *n*BuLi and subsequent trapping with TMSCl proved inefficient,[38] but treatment with CF_3TMS in the presence of a catalytic amount of CsF[39] proceeded cleanly to convert (*R*)-**11** into the desired product (*S*)-**12** in good yield (80%) [Note: the change in the *R* to the *S* assignment here is the result of silylation of the ethynyl end of the molecule, which reverses the Cahn–Ingold–Prelog priority around the stereogenic center]. Under stringently oxygen-free conditions, cross-coupling between (*S*)-**12** and phenylacetylene furnished (*S*)-**13** (Scheme 5).

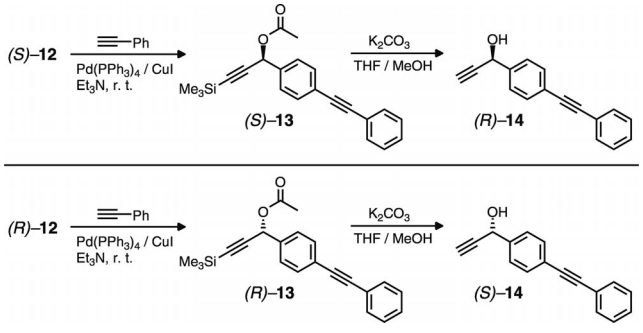

Scheme 5. Installation of linear π-conjugation on an enantiomeric pair of aryl propargylic alcohols.

Removal of the trimethylsilyl and acyl groups was conveniently achieved in a one-step procedure with K_2CO_3 in a mixed solvent (THF/MeOH) to afford (*R*)-**14**. The synthesis of the enantiomeric alcohol (*S*)-**14** was carried out from (*R*)-**12** in a similar manner. The latter compound was prepared by acetylation and TMS-protection of (*S*)-**10** as shown in Scheme 4 and subjected to cross-coupling with phenylacetylene followed by deprotection to furnish (*S*)-**14**.

Synthesis of the branched phenylene(ethynylene) fragment (*R*)-**20** (Scheme 6), for incorporation into $(S)_3$-**5** and $(S,S)_3$-**6** (Figure 3), began with a Sonogashira–Hagihara coupling between tribromobenzene and 2-methylbut-3-yn-2-ol (**15**).[40] The presence of the OH group in this "acetone-protected" acetylene equivalent aided the separation of **16** from doubly and triply coupled byproducts as well as unreacted starting materials, each of which has distinctively different polarity. The monocoupling product **16** was isolated and subjected to coupling with an excess amount (3 equiv.) of phenylacetylene to obtain **17**. The tertiary alcohol group in **17** was removed by treatment with KOH in toluene at reflux to yield the free alkyne **18**, which was subjected to cross-coupling with (*S*)-**12**. Removal of the trimethylsilyl and acetyl groups from the coupling product (*S*)-**19** completed the synthesis of (*R*)-**20**.

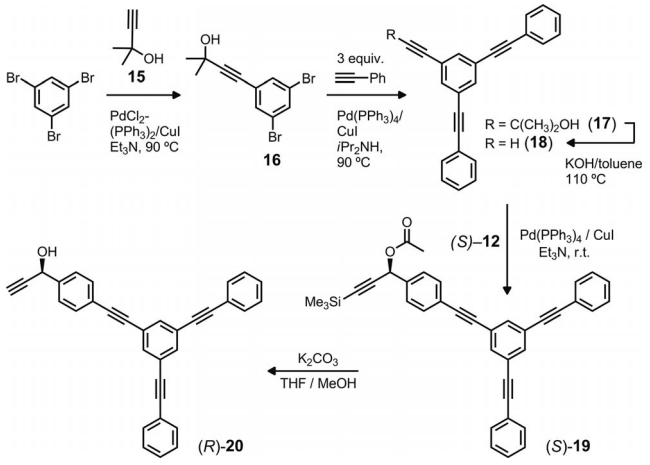

Scheme 6. Installation of branched π-conjugation onto the chiral propargylic alcohol.

Construction of *Chiral Blades* for C_3-Symmetric Propeller-Shaped Molecules

With efficient synthetic routes for the propargylic alcohols (*R*)-**14**, (*S*)-**14**, and (*R*)-**20** established, we proceeded to prepare a series of "propeller blades". The design of the molecules **21**–**25** (Figure 4) specifically took account of

i) mono- (**21** and **24**) versus disubstitution (**22**, **23**, and **25**) on the aniline ring to set the number of chiral centers and hydrogen bonds (Figure 3),

ii) absolute configurations (i.e., *R* vs. *S*) of the chiral alcohol groups to control the preferred directionality of folding (Figure 1), and

iii) linear (**21**, **22**, and **23**) versus branched (**24** and **25**) elongation of π-conjugation to modulate the degree of steric bias for asymmetric folding (Figure 1 and Figure 2)

in the resulting C_3-symmetric chiral molecules listed in Figure 3.

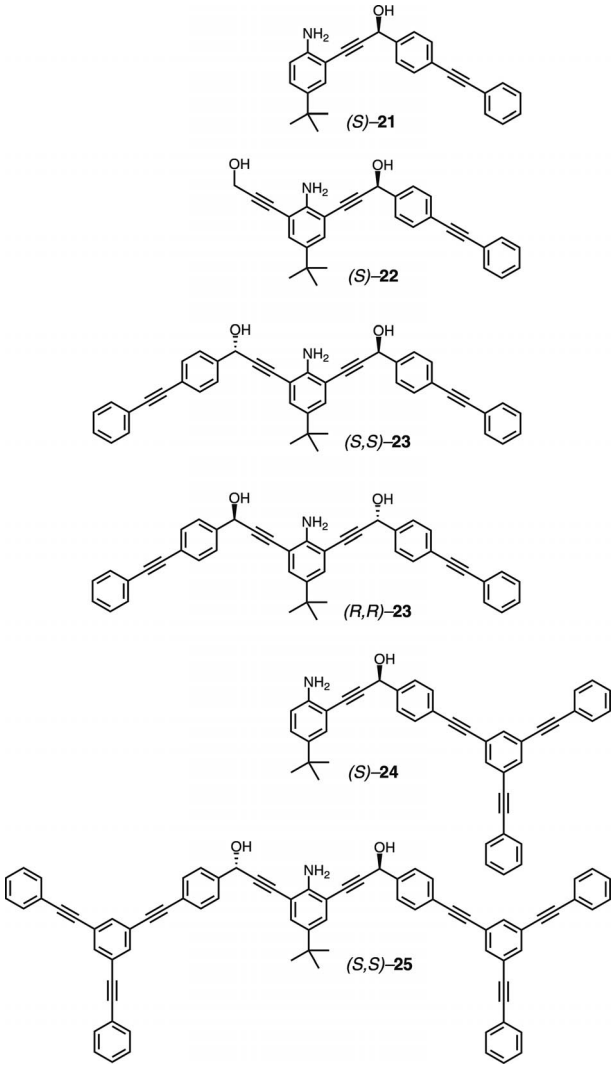

Figure 4. Chemical structures of chiral amine derivatives.

Preparation of these chiral anilines was achieved in a straightforward manner through cross-coupling reactions between the propargylic alcohols and either monoiodoaniline (**26**) or diiodoaniline (**27**). As summarized in Scheme 7, **route I** was taken for (*S*)-**21** and (*S*)-**24**, which were subjected to efficient triple Schiff base condensation reactions with 1,3,5-triformylphloroglucinol (**28**) to furnish $(S)_3$-**3** and $(S)_3$-**5** (Figure 3), respectively. The asymmetrically 2,6-disubstituted aniline (*S*)-**22** was prepared by consecutive cross-coupling of the diiodoaniline **27** with propargyl alcohol and with (*R*)-**14**, and carried forward to the triple condensation product $(S)_3$-**7** (Scheme 7, **route II**). With the 2,6-disubstituted anilines (*S*,*S*)-**23**, (*R*,*R*)-**23**, and (*S*,*S*)-**25**, **route III** was followed to prepare the triple Schiff base adducts $(S,S)_3$-**4**, $(R,R)_3$-**4**, and $(S,S)_3$-**6**, respectively.

When the reactions were carried out in EtOH at reflux, the aromatic-rich triple Schiff base condensation products precipitated out of the polar reaction mixtures. In most cases, analytically pure products could be isolated by simple filtration and repeated washing, without resort to chromatographic separation.

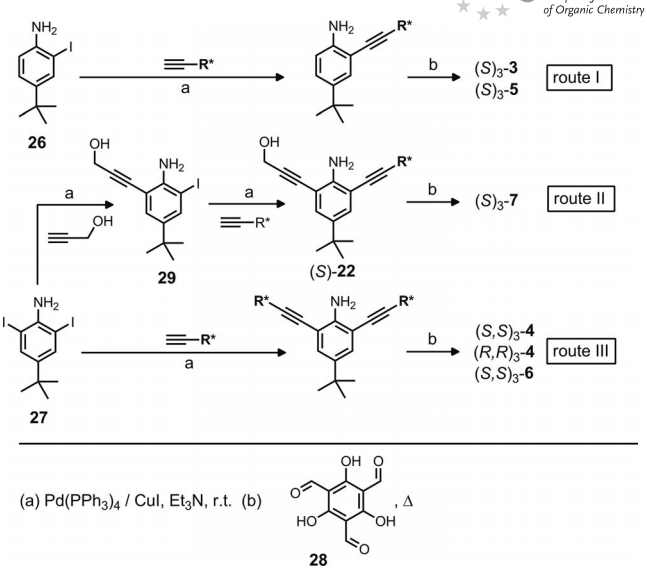

Scheme 7. Synthetic routes to monosubstituted and disubstituted anilines and their incorporation into the chiral tris(*N*-salicylidenamine)s.

Hydrogen-Bonding-Assisted Structural Folding

In $CDCl_3$ at T = 298 K, compounds **1**–**7** (Figure 3) each show a simple ^{1}H NMR pattern consistent with molecular threefold symmetry. A set of doublets at 14.01–13.34 ppm and 9.64–8.77 ppm, assigned to the $N_{enamine}$–H and C_{vinyl}–H protons, respectively, is consistent with the keto–enamine, rather than enol–imine, description of the core tautomerism.[20,25–27] This assignment is supported further by the carbonyl ^{13}C NMR resonances at ca. 185 ppm observed across the entire series **1**–**7**, and by their achiral analogues, for which X-ray structures are available.[25a–25c,25e–25g] In particular, the observation of only one set of N–H and C–H resonances in each case here supports the notion that each solution population is dominated by a single geometrical isomer of *pseudo*-C_3 symmetry, which maximizes the number of energy-stabilizing N–H···O hydrogen bonds at the core and O–H···O–H hydrogen bonds between the wingtip alcohol groups (Figure 3). Synthesis of tris(*N*-salicylidenamine)s lacking such noncovalent interactions often results in inseparable mixtures of *two* isomers as shown in Equation (1).[26,27]

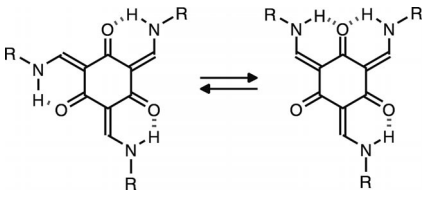

(1)

In order to probe hydrogen-bonding assisted structural folding in solution further, a 2D-ROESY NMR spectrum for $(S)_3$-**7** in $CDCl_3$ at 298 K was obtained (Figure 5). Multiple crosspeaks were observed between C_{vinyl}–H/$N_{enamine}$–H at the tris(*N*-salicylidenamine) core and O–H protons of both primary and secondary propargylic groups. In ad-

dition, crosspeaks of opposite phase were observed for OH···OH, relative to those of CH···OH and NH···OH, indicating chemical exchange in solution.[41] These spectroscopic signatures give support for the formation of a helical conformation in solution that brings adjacent (but belonging to different peripheral aryl groups) wingtip OH groups into close proximity, to effectively "flatten" the entire structure and to establish conformationally rigid spatial relationships. 2D-ROESY NMR studies on the phenyl-substituted analogue[20] provided evidence of similar structural folding in solution.

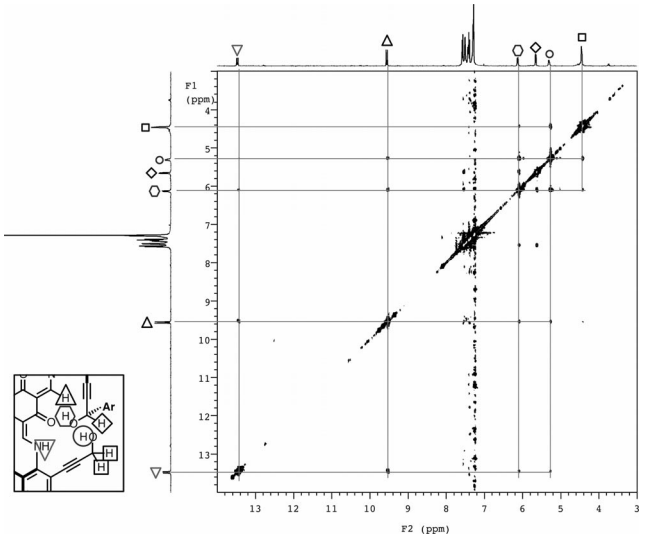

Figure 5. 2D-ROESY spectrum of $(S)_3$-**7** in $CDCl_3$ at T = 298 K, and a close-up view of the chemical structure with protons contributing to ROE and TOCSY-relayed ROE cross-peaks labeled with symbols that correspond to the assigned resonances in the 1-D spectra.

Across the entire series **1**–**7**, the formation of intramolecular O–H···O hydrogen bonds is manifested most prominently by the propargylic O–H proton resonances at δ = 6.09–6.25 ppm, which are shifted significantly downfield in relation to that (δ = 2.27 ppm) of the model compound **8**. A narrow distribution of this parameter ($\Delta\delta$ = 0.16 ppm over eight different systems) indicates that the introduction of bulky aryl groups at the wingtips does not deleteriously affect the stabilities of the conformations of the folded forms. This observation further supports the computational models shown in Figures 1 and 2. In the "correctly folded" form, substituents at the *para*-positions of the wingtip phenyl rings point *away* from the molecular cores and therefore should not deleteriously affect the thermodynamic stabilities of the systems. The spatial arrangements of these π-extended groups and their collective effects on the preferred handedness of the propeller-shaped molecular cores were probed further by UV/Vis and CD spectroscopy.

Conformational Bias and Asymmetric Folding Probed by UV/Vis and CD Spectroscopy

With ^{1}H NMR spectroscopic evidence for structural folding in solution in hand, we decided to employ UV/Vis and CD studies to probe its consequences on i) the electronic structures of the [n,π]-conjugated molecular cores, and ii) interchromophore electronic coupling between π-extended wingtip groups that are brought into close proximity through O–H···O–H hydrogen bonds between the wingtips.

As shown in Figure 6, the UV/Vis spectrum of $(S,S)_3$-**4** in $CHCl_3$ is characterized by broad longer-wavelength absorptions at λ = 400–450 nm and intense high-energy transitions at λ = 270–310 nm. Extensive TD-DFT studies on the parent $(S,S)_3$-**2** system (with the simple phenyl group as substituent on the wingtip alcohol group) have previously established that the features at λ = 400–450 nm are associated with the [n,π]-conjugated tris(*N*-salicylidenaniline) core part of the molecule.[20] In support of this notion, the UV/Vis spectra of $(S,S)_3$-**2** and $(S,S)_3$-**4** are essentially superimposable in this energy window (Figure 6, a). On the other hand, the intensities (ε = 2.0×10^5 to 2.2×10^5 $M^{-1}cm^{-1}$) of the shorter wavelength absorptions of $(S,S)_3$-**4** at λ = 270–310 nm are markedly enhanced and slightly red-shifted from those of $(S,S)_3$-**2**, suggesting that they originate from the (phenylethynyl)phenyl fragments attached to the wingtip alcohol groups. Indeed, $(S)_3$-**3** displays very similar absorptions at λ = 270–310 nm but with half the intensities (ε = 8.4×10^4 to 1.1×10^5 $M^{-1}cm^{-1}$) of $(S,S)_3$-**4** (Figure 6, a), which establishes a direct correlation between the molar absorptivity and the number of the local chromophores [i.e., six for $(S,S)_3$-**4** vs. three for $(S)_3$-**3**]

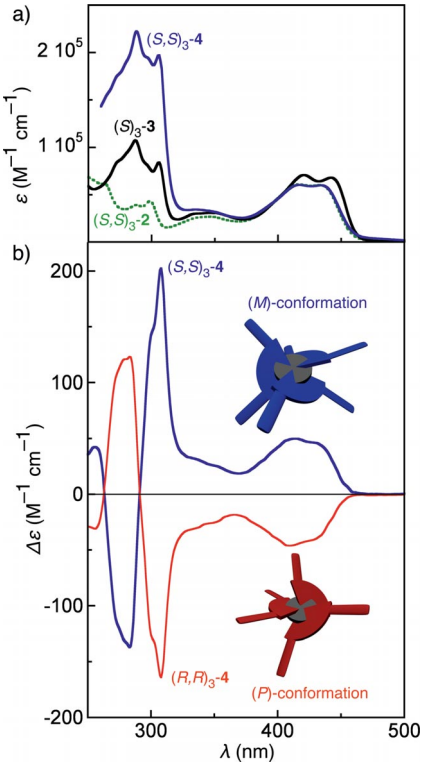

Figure 6. a) UV/Vis spectra of $(S,S)_3$-**2** (green), $(S)_3$-**3** (black), and $(S,S)_3$-**4** (blue) in $CHCl_3$. b) CD spectra of $(S,S)_3$-**4** (blue) and $(R,R)_3$-**4** (red) in $CHCl_3$, along with schematic presentations of preferred handedness of folding. See Figure 8 for the assignment of absolute screw sense from the bisignate CD feature across λ = 292 nm. T = 298 K.

within the molecule. Effective decoupling between the electronic structure of the molecular core (responsible for the absorption at λ = 400–450 nm) and the peripheral π-conjugation (responsible for the absorption at λ = 270–310 nm) is thus confirmed in a straightforward manner. The absence of direct conjugation between the two chromogenic components was fortuitous for simplification of our subsequent data analysis.

The CD spectrum of $(S,S)_3$-**4** in $CHCl_3$ (Figure 6, b) has positive Cotton signals at the longer-wavelength end. Under similar conditions, the enantiomeric $(R,R)_3$-**4** produces a mirror-image spectrum and hence a reversal in this signal (Figure 6, b). Our previous benchmark TD-DFT studies have established that this CD feature signifies the predominance of one screw sense of the propeller molecule, which for $(S,S)_3$-**2** in solution is the *M* conformer.[20] Such an assignment is now further validated by the bisignate CD feature of $(S,S)_3$-**4** toward the shorter-wavelength end (with positive band at λ = 308 nm and negative band λ = 283 nm). A detailed analysis of the interchromophore exciton coupling, which is responsible for this phenomenon, is provided in the following section.

An effective transfer of the *S* central chirality present *at the peripheral wingtips* to the *M* helical chirality *of the propeller-shaped molecular core* is maintained across the entire series **1**–**7**, as reflected in the consistently positive Cotton signals at $\lambda > 350$ nm (Figure S3 in the Supporting Information). Although such a correlation supports the general applicability of the chiral induction model shown in Figures 1 and 2, the absolute magnitude of this signature feature depends critically on the structural contexts in which the individual chiral fragments are located. As shown in Scheme 2, chiral tris(*N*-salicylidenaniline)s can switch between the *M* and *P* conformations through correlated tilting motions of the peripheral aryl groups. The CD signal from the core chromophore thus reflects the difference in the relative stabilities of the two conformations of opposite screw sense, which is determined both by the size and by the number of chiral groups that are brought into close proximity upon structural folding.

As shown in Figure 7, the CD signal intensity of $(S,S)_3$-**4** at 415 nm ($\Delta\varepsilon_{415}$) in $CHCl_3$ is 50 $M^{-1}cm^{-1}$, which is about 2.5 times larger than that (21 $M^{-1}cm^{-1}$) of $(S,S)_3$-**2** under similar conditions. These two molecules have structural skeletons that are identical except for the substituents on the wingtip alcohol groups: linearly π-extended (phenylethynyl)phenyl for $(S,S)_3$-**4** versus simple phenyl for $(S,S)_3$-**2** (Figure 3). In the preferred *M* conformation adopted both by $(S,S)_3$-**2** and by $(S,S)_3$-**4**, these aryl groups point away from the molecular cores (see Figures 1 and 2) and are therefore less likely to affect the overall stabilities of the molecules. In the competing *P* conformation (denoted the "misfolded" form in our design rationale; Figure 1), however, they converge at the congested molecular cores. As a consequence, the energy penalty becomes more severe for the bulkier (phenylethynyl)phenyl groups in $(S,S)_3$-**4** than for the simple phenyl groups in $(S,S)_3$-**2** (see Figures 1 and 2).[42]

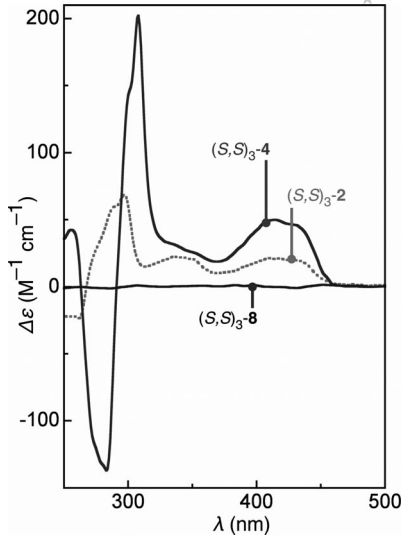

Figure 7. CD spectra of $(S,S)_3$-**2**, $(S,S)_3$-**4**, and $(S,S)_3$-**8** in $CHCl_3$ at *T* = 298 K.

The enhanced conformational stability of $(S,S)_3$-**4** relative to $(S,S)_3$-**2** thus derives not so much from the stabilization of the preferred conformer as from the destabilization of the less-preferred conformer, which is the hallmark of *negative design*. A similar increase in $\Delta\varepsilon_{415}$ was also observed upon installation of 3,5-bis(ethynylenephenyl) substituents on the $(S,S)_3$-**4** system to produce the sterically more congested $(S,S)_3$-**6** (see Figure S3a in the Supporting Information). The larger positive Cotton effects observed for $(S)_3$-**3** ($\Delta\varepsilon_{415}$ = 31 $M^{-1}cm^{-1}$) and $(S)_3$-**5** ($\Delta\varepsilon_{415}$ = 33 $M^{-1}cm^{-1}$) relative to $(S)_3$-**1** ($\Delta\varepsilon_{415}$ = 19 $M^{-1}cm^{-1}$) also corroborate this structure–property model (see Figure S3b).

In addition to specific chemical structures, the sheer number of chirality-transferring groups within a molecule plays a critical role in the selection and stabilization of the preferred conformation. As shown in Figure 3, $(S,S)_3$-**4** and $(S)_3$-**7** have the same number of O–H···O–H hydrogen bonding contacts but different numbers of chiral propargylic alcohol groups. For both systems, positive Cotton effects were observed in the longer-wavelength end. The magnitude of this signal, however, essentially increases fivefold from $\Delta\varepsilon_{415}$ = 9 $M^{-1}cm^{-1}$ for $(S)_3$-**7** (with three chiral alcohol groups) to $\Delta\varepsilon_{415}$ = 50 $M^{-1}cm^{-1}$ for $(S,S)_3$-**4** (with six chiral alcohol groups) (Figure S3). This phenomenon reflects an increased steric bias towards the *M* conformation with increasing number of pairwise contacts between chiral wingtip groups upon structural folding.

The stereoinduction mechanism discussed above operates through tight O–H···O hydrogen bonding networks that effectively transmit point chirality present at the molecular perimeter to the helical twisting of the molecular core. The importance of such noncovalent contacts as "conduits" for intramolecular chirality transfer was probed by solvent-dependent CD studies. As shown in Figure 8, the positive Cotton effects ($\Delta\varepsilon_{420}$) of the compound $(S,S)_3$-**4** show a systematic decrease in signal intensity with increasing solvent donor number (DN).[43] This observation corroborates the

notion that disruption of the intramolecular O–H···O contacts by Lewis basic (and also hydrogen-bond accepting) solvents leads to an effective "unfolding" of the molecule with loss of well-defined secondary structures. Intriguingly, a further increase in DN led to an *inversion* of the sign in the Cotton effect of $(S,S)_3$-**4** in DMF, DMA, and DMSO (Figure 8). Similar behavior had previously been reported for $(S,S)_3$-**2**,[20] and was interpreted as the consequence of O–H···(solvent)$_n$ interactions in strong donor solvents that provide sufficient steric bias to reorient the electronic transition dipoles and give rise to *pseudo*-mirror image CD signals. Qualitatively consistent solvent-dependent spectral changes were observed for $(S,S)_3$-**6**, $(S)_3$-**3**, and $(S)_3$-**5** (Figure S5), which suggests a general applicability of this empirical model for chiral tris(*N*-salicylidenaniline)s.

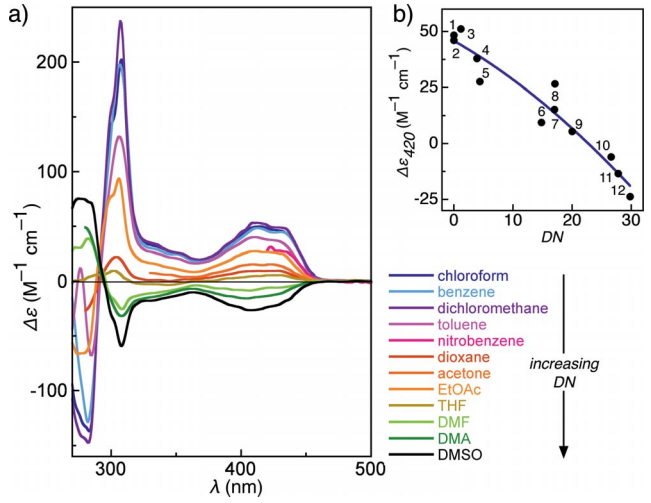

Figure 8. a) Solvent-dependent changes in the CD spectrum of $(S,S)_3$-**4** at T = 298 K. Because of strong background absorption, data in nitrobenzene were obtained only at >420 nm. b) Plots of $\Delta\varepsilon_{420}$ ($\Delta\varepsilon$ at 420 nm) of $(S,S)_3$-**4** versus donor number (DN) for solvents including chloroform (1), benzene (2), dichloromethane (3), toluene (4), nitrobenzene (5), dioxane (6), acetone (7), ethyl acetate (8), THF (9), DMF (10), DMA (11), and DMSO (12).

Exciton-Coupled Circular Dichroism (ECCD)

A salient feature of the CD spectrum of $(S,S)_3$-**4** (Figure 6) is the *bisignate* pattern that changes its sign *from positive to negative* toward the shorter-wavelength end of the spectral window. The reference system $(S,S)_3$-**2** shows a similar change in the sign of the Cotton effects (Figure 7). The crossover wavelength of λ = 267 nm for $(S,S)_3$-**2**, however, lies closer to the high-energy end without full development of the negative band, thus making the bisignate feature less pronounced. A linear elongation of the π-conjugation in $(S,S)_3$-**4**, on the other hand, produces significant red shifts in this spectral region (Figure 6, b) to reveal a well-defined bisignate CD couplet across λ = 292 nm (Figure 7), which is characteristic of exciton coupling.

Exciton coupling results from through-space interaction between multiple chromophores that have strong electric dipole-allowed transitions.[28] When such interactions occur between two equivalent (= energetically degenerate) chromophores, the excited states split into two energy levels to broaden the UV/Vis absorption band. A more pronounced, and thus practically useful, signature of this phenomenon is "splitting" of the CD signal as shown in Figure 7. The change in the sign of such a coupled CD signal, either positive-to-negative (positive CD couplet) or negative-to-positive (negative CD couplet), correlates directly with the absolute sense of torsion between two electric transition dipoles that are brought into close proximity in space.[28] This exciton chirality rule establishes a robust structure–spectra relationship that has been used extensively in the stereochemical analysis of natural products,[28] and chiral alcohols, amines, and aminols.[44,45] A particularly relevant example in this context is the use of ECCD to assign the absolute directionality of unidirectional rotary movements of molecular motors constructed with sterically overcrowded alkenes.[22,46]

The CD couplet of $(S,S)_3$-**4** is centered at λ = 292 nm (Figure 7), which is close to the λ_{max} = 279 nm of the diphenylacetylene π–π* transition.[47,48] Exciton coupling here thus arises from two (phenylethynyl)phenyl chromophores that are brought into close proximity through O–H···O–H contacts (Figure 2). The experimentally observed positive CD couplet (Figure 7) of $(S,S)_3$-**4** thus dictates a positive chirality (= clockwise torsional relationship) of two electric transition dipoles, each of which lies parallel to the long axis of the π-conjugation (Figure 9, a). This spectroscopic

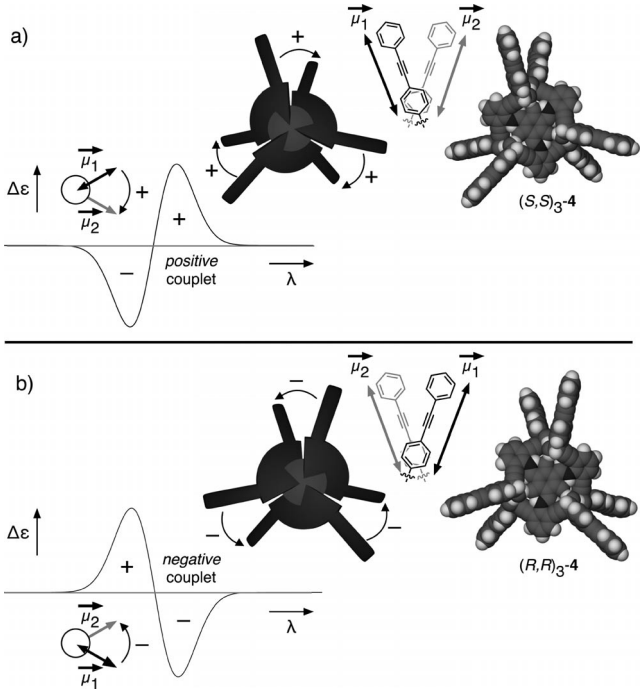

Figure 9. Bisignate CD curves arising from exciton coupling of two identical chromophores with a) positive and b) negative chirality, as defined by the spatial relationship between the two interacting electric transition dipoles μ_1 and μ_2. Shown next to each CD curve are space-filling models of a) $(S,S)_3$-**4** and b) $(R,R)_3$-**4**, and cartoon-type representations highlighting the relative orientations of the coupled π–π* transitions of the diphenylacetylene chromophores.

interpretation is fully consistent with the PM3 energy-minimized structure of $(S,S)_3$-**4** shown in Figure 2. For the enantiomeric $(R,R)_3$-**4**, this spatial relationship is reversed to a negative chirality (Figure 9, b), which translates to the experimentally observed negative CD couplet (Figure 6, b).

Comparative CD spectroscopic studies on the series $(S,S)_3$-**4**, $(S)_3$-**7**, and $(S,S)_3$-**8** further sharpened our understanding of the exciton coupling. The model compound $(S)_3$-**7** also has (phenylethynyl)phenyl fragments as in $(S,S)_3$-**4**, but their large spatial separation produces a weakly coupled CD signal with A_{CD} (= amplitude of the CD exciton couplet = difference in $\Delta\varepsilon$ between the peak and the trough) = 40 $M^{-1}cm^{-1}$, in comparison with A_{CD} = 340 $M^{-1}cm^{-1}$ in the case of $(S,S)_3$-**4** (Figure S3a in the Supporting Information). The C_2-chiral subunit model (*S*,*S*)-**8** has two (phenylethynyl)phenyl fragments across the 2,6-diethynylphenylene backbone, but no exciton-coupled feature was observed in its CD spectrum (Figure 7). In the absence of an appropriate conformational lock, the molecule samples a large conformational space through unrestricted C–C bond rotations. Consequently, (*S*,*S*)-**8** fails to produce a well-defined absolute sense of twist that is critical for exciton coupling. In a similar fashion, chiral secondary structures display stronger ECCD intensities relative to their random-coil analogues.[13d,18f,19b]

The strongly coupled CD signal of $(S,S)_3$-**4** thus arises from close positioning of multiple π-extended chromophores that are brought into conformationally rigid chiral environments through a tight O–H···O–H hydrogen bonding network (Figure 2). In support of this notion, a similarly intense (A_{CD} = 300 $M^{-1}cm^{-1}$) positive CD couplet was observed for $(S,S)_3$-**6** containing additional 3,5-bis(phenylethynyl) substituents (Figure S3a in the Supporting Information). Apparently, the *meta* linkage in the branched π-conjugation in $(S,S)_3$-**6** gives rise to π–π* transitions that are localized to the (phenylethynyl)phenyl fragment as in $(S,S)_3$-**4**, and produces similar exciton-coupled CD patterns.

As shown in Figure 8, the solvent-dependent changes in the ECCD signal of $(S,S)_3$-**4** at the shorter-wavelength end (reflecting changes in the interchromophore coupling at the "propeller blade tips") correlate nicely with changes in the Cotton effects in the longer-wavelength region (reflecting changes in the handedness of the "propeller core"). This observation is a compelling manifestation of the principle that local bond twisting motions can be correlated and effectively transmitted to remote locations with the molecule through rigid π-skeletons.

Conclusions

We have prepared a series of chiral tris(*N*-salicylidenaniline)s and have investigated their solution dynamics leading to helical folding. The assembly of these C_3-symmetric propeller-shaped molecules was aided by synthetic access to new chiral propargylic alcohols through enzymatic kinetic resolution and C–C cross-coupling reactions. Notably, this synthetic strategy facilitated the incorporation of a wide range of steric and electronic controller groups on a versatile chiral scaffold that guides hydrogen bonding with preferred handedness. The stability of a cyclic array of O–H···O–H contacts located in such a structural setting is reinforced further by molecular threefold symmetry, the absolute screw sense (i.e., *P* vs. *M*) of which is dictated by the absolute configuration (i.e., *R* vs. *S*) of the chiral alcohol groups. Phenyleneethynylene-based π-conjugated substituents attached to these stereogenic centers support well-defined electric transition dipoles, the torsional relationships of which assisted assignment of the absolute screw sense of structural folding by exciton-coupled bisignate CD signals.

Our comparative spectroscopic studies have established that this *central-to-helical chirality transfer* model is generally applicable to a large set of tris(*N*-salicylidenaniline) derivatives, the conformational stabilities of which depend critically on i) the number of hydrogen bonds and ii) the steric demands of the extended π-conjugation introduced at the chiral "wingtips". In particular, the principles of *negative design* were successfully implemented here to enhance the solution populations of individual helical conformations by destabilizing "misfolded" conformations.

Experimental Section

General: All reagents were obtained from commercial suppliers and used as received unless otherwise noted. All air-sensitive manipulations were carried out under nitrogen by standard Schlenk-line techniques. Tetrahydrofuran and dichloromethane were saturated with nitrogen and purified by passage through activated Al_2O_3 columns under nitrogen (Innovative Technology SPS 400).[49] Compounds $(S)_3$-**1**,[20] $(S,S)_3$-**2**,[20] **9**,[35a] **16**,[40] **26**,[50] **27**,[51] and **28**[26a] were synthesized by literature procedures.

Physical Measurements: Proton nuclear magnetic resonance (^{1}H NMR) spectra were measured with a Varian INOVA-400 (400 MHz) or Varian Gemini 2000 (300 MHz) NMR spectrometer at T = 298 K unless otherwise noted. Carbon nuclear magnetic resonance (^{13}C NMR) spectra were measured with a Varian INOVA-400 (100 MHz) spectrometer at T = 298 K unless otherwise noted. ^{1}H NMR and ^{13}C NMR spectra were acquired as solutions in $CDCl_3$ and are reported in parts per million (ppm) downfield (δ) from tetramethylsilane with use of residual chloroform ($CHCl_3$) as an internal standard set to δ = 7.26 ppm (for ^{1}H NMR) and 77.16 ppm (for ^{13}C NMR). Proton NMR spectroscopic data are reported in the form: δ (multiplicity, coupling constants, number of protons). High-resolution mass spectral (HR-MS) data were obtained with a Thermo Electron Corporation MAT 95XP-Trap instrument. MALDI-TOF mass spectroscopic data were collected with a Bruker Biflex III instrument. FT-IR spectra were recorded with a Nicolet 510P FT-IR spectrometer with EZ OMNIC ESP software. UV/Vis spectra were recorded with an Agilent 8453 UV/Vis spectrophotometer with ChemStation. Circular dichroism spectra were recorded with a Jasco J-715 circular dichroism spectrometer. Chiral HPLC was monitored with a Waters dual λ absorbance detector with a chiral column [Regis, Pirkle Covalent, (*S*,*S*)-Whelk-O 1, 25 cm × 4.6 mm].

(2*E*,4*E*,6*E*)-2,4,6-Tris[(4-*tert*-butyl-2-{(*S*)-3-hydroxy-3-[4-(phenylethynyl)phenyl]prop-1-ynyl}phenylamino)methylene]cyclohexane-

1,3,5-trione [$(S)_3$-3]: An EtOH (8.2 mL) solution of (*S*)-**21** (0.250 g, 0.66 mmol) was purged with N_2 for 10 min. A portion of **28** (0.035 g, 0.17 mmol) was added and the mixture was heated at reflux for 12 h. A yellow solid was isolated by filtration and washed with pentanes to afford $(S)_3$-**3** (0.167 g, 77%). ^{1}H NMR (300 MHz, $CDCl_3$): δ = 14.60 (d, J = 13.2 Hz, 3 H), 8.77 (d, J = 13.4 Hz, 3 H), 7.69 (d, J = 8.1 Hz, 6 H), 7.58 (d, J = 8.3 Hz, 6 H), 7.52–7.50 (m, 6 H), 7.38–7.27 (m, 18 H), 6.23 (d, J = 5.4 Hz, 3 H), 5.84 (d, J = 5.6 Hz, 3 H), 1.26 (s, 27 H) ppm. ^{13}C NMR (100 MHz, $CDCl_3$): δ = 217.2, 184.6, 148.5, 147.8, 141.3, 137.9, 131.9, 131.7, 128.5 (2 peaks), 127.6, 127.0, 123.3, 123.1, 113.0, 106.7, 97.5, 89.7, 89.3, 64.7, 34.6, 31.2, 29.8 ppm. FT-IR (thin film on NaCl): $\tilde{\nu}$ = 3366, 3059, 2964, 2902, 2865, 2183, 1618, 1597, 1451, 1345, 1300, 1231, 984, 754 cm^{-1}. MS (MALDI-TOF) calcd. for $C_{90}H_{75}N_3O_6Na$ 1316.555 $[M + Na]^+$; found 1316.631.

(2*E*,4*E*,6*E*)-2,4,6-Tris[(4-*tert*-butyl-2,6-bis{(*S*)-3-hydroxy-3-[4-(phenylethynyl)phenyl]prop-1-ynyl}phenylamino)methylene]cyclohexane-1,3,5-trione [$(S,S)_3$-4]: An EtOH (6.0 mL) solution of (*S*,*S*)-**23** (0.250 g, 0.41 mmol) was purged with N_2 for 10 min. A portion of **28** (0.022 g, 0.10 mmol) was added and the mixture was heated at reflux for 16 h. A yellow solid was isolated by filtration and washed with EtOH to furnish $(S,S)_3$-**4** (0.11 g, 53%). ^{1}H NMR (400 MHz, $CDCl_3$): δ = 13.34 (d, J = 13.5 Hz, 3 H), 9.39 (d, J = 13.3 Hz, 3 H), 7.54 (d, J = 8.2 Hz, 12 H), 7.49 (s, 6 H), 7.39 (d, J = 8.4 Hz, 12 H), 7.36 (dd, J = 8.0, 1.6 Hz, 15 H), 7.25–7.19 (m, 15 H), 5.53 (s, 6 H), 1.33 (s, 27 H) ppm. ^{13}C NMR (100 MHz, $CDCl_3$): δ = 185.1, 151.9, 148.6, 140.5, 138.4, 131.7, 131.6, 131.2, 128.3, 127.0, 123.3, 123.1, 113.8, 106.4, 96.6, 89.9, 89.3, 82.7, 64.4, 34.7, 31.2, 29.9 ppm. FT-IR (thin film on NaCl): $\tilde{\nu}$ = 3368, 3059, 2964, 2903, 2868, 2217, 1602, 1570, 1507, 1432, 1402, 1365, 1301, 1233, 1097, 1027, 984, 910, 841, 785, 754, 733, 689, 645, 596, 464 cm^{-1}. MS (MALDI-TOF) calcd. for $C_{141}H_{105}N_3O_9Na$ 2008.782 $[M + Na]^+$; found 2008.031.

(1*S*,1′*S*)-3,3′-(1,3-Phenylene)bis{1-[4-(phenylethynyl)phenyl]prop-2-yn-1-ol} [(*S*,*S*)-8]: A Teflon screw-capped tube was loaded with 1,3-diiodobenzene (0.13 g, 0.39 mmol), $Pd(PPh_3)_4$ (0.009 g, 0.008 mmol), and CuI (0.002 g, 0.012 mmol). The reaction vessel was evacuated and back-filled three times with N_2. A portion of Et_3N (6 mL) was added under N_2. The vessel was sealed and the reaction mixture was stirred at room temp. for 16 h. Flash column chromatography on SiO_2 (hexanes/EtOAc 2:1, v/v) afforded (*S*,*S*)-**8** as a peach solid (0.19 g, 88%). ^{1}H NMR (300 MHz, $CDCl_3$): δ = 7.60–7.53 (m, 13 H), 7.45 (dd, J = 7.8, 1.6 Hz, 2 H), 7.37–7.28 (m, 7 H), 5.70 (d, J = 6.1 Hz, 2 H), 2.27 (d, J = 6.1 Hz, 2 H) ppm. ^{13}C NMR (100 MHz, $CDCl_3$): δ = 140.5, 135.1, 132.1, 132.0, 131.8, 129.7, 128.6, 128.5, 126.8, 123.7, 123.3, 122.8, 90.1, 89.2, 89.1, 86.1, 64.9 ppm. FT-IR (thin film on NaCl): $\tilde{\nu}$ = 3300, 2201, 1635, 1594, 1507, 1476, 1406, 1299, 1183, 1037, 987, 906, 844, 790, 753, 683, 517 cm^{-1}. MS (HR-CI) calcd. for $C_{40}H_{26}O_2$ $[M]^+$ 538.1933; found 538.1921.

Supporting Information (see footnote on the first page of this article): Experimental details for synthesis and additional spectroscopic data.

Acknowledgments

This work was supported by the National Science Foundation (NSF) (CAREER CHE 0547251) and the U.S. Army Research Office (W911NF-07-1-0533). We thank Dr. András Olasz for assistance in computational studies.

[1] a) S. H. Gellman, *Acc. Chem. Res.* **1998**, *31*, 173–180; b) D. J. Hill, M. J. Mio, R. B. Prince, T. S. Hughes, J. S. Moore, *Chem. Rev.* **2001**, *101*, 3893–4011; c) B. Gong, *Chem. Eur. J.* **2001**, *7*, 4336–4342; d) R. P. Cheng, S. H. Gellman, W. F. DeGrado, *Chem. Rev.* **2001**, *101*, 3219–3232; e) C. Schmuck, *Angew. Chem.* **2003**, *115*, 2552; *Angew. Chem. Int. Ed.* **2003**, *42*, 2448–2452; f) R. P. Cheng, *Curr. Opin. Struct. Biol.* **2004**, *14*, 512–520; g) I. Huc, *Eur. J. Org. Chem.* **2004**, 17–29; h) D. Seebach, D. F. Hook, A. Glättli, *Biopolymers* **2006**, *84*, 23–37; i) M. T. Stone, J. M. Heemstra, J. S. Moore, *Acc. Chem. Res.* **2006**, *39*, 11–20; j) A. D. Bautista, C. J. Craig, E. A. Harker, A. Schepartz, *Curr. Opin. Chem. Biol.* **2007**, *11*, 685–692; k) C. M. Goodman, S. Choi, S. Shandler, W. F. DeGrado, *Nat. Chem. Biol.* **2007**, *3*, 252–262; l) W. S. Horne, S. H. Gellman, *Acc. Chem. Res.* **2008**, *41*, 1399–1408; m) X. Li, Y.-D. Wu, D. Yang, *Acc. Chem. Res.* **2008**, *41*, 1428–1438; n) Z.-T. Li, J.-L. Hou, C. Li, *Acc. Chem. Res.* **2008**, *41*, 1343–1353; o) B. Yoo, K. Kirshenbaum, *Curr. Opin. Chem. Biol.* **2008**, *12*, 714–721; p) I. Saraogi, A. D. Hamilton, *Chem. Soc. Rev.* **2009**, *38*, 1726–1743; q) H. Juwarker, J.-m. Suk, K.-S. Jeong, *Chem. Soc. Rev.* **2009**, *38*, 3316–3325; r) C. A. Olsen, *ChemBioChem* **2010**, *11*, 152–160; s) G. N. Tew, R. W. Scott, M. L. Klein, W. F. DeGrado, *Acc. Chem. Res.* **2010**, *43*, 30–39; t) X. Zhao, Z.-T. Li, *Chem. Commun.* **2010**, *46*, 1601–1616.

[2] S. Hecht, I. Huc, *Foldamers*, Wiley-VCH, Weinheim, Germany, **2007**.

[3] For a special thematic issue on peptidomimetics, see: *Acc. Chem. Res.* **2008**, *41*, 1231–1438.

[4] a) C. M. Dobson, *Nature* **2003**, *426*, 884–890; b) K. A. Dill, S. B. Ozkan, M. S. Shell, T. R. Weikl, *Annu. Rev. Biophys.* **2008**, *37*, 289–316.

[5] a) M. H. Hecht, J. S. Richardson, D. C. Richardson, R. C. Ogden, *Science* **1990**, *249*, 884–891; b) J. J. Havranek, P. B. Harbury, *Nat. Struct. Biol.* **2003**, *10*, 45–52.

[6] a) W. F. DeGrado, C. M. Summa, V. Pavone, F. Nastri, A. Lombardi, *Annu. Rev. Biochem.* **1999**, *68*, 779–819; b) R. B. Hill, D. P. Raleigh, A. Lombardi, W. F. DeGrado, *Acc. Chem. Res.* **2000**, *33*, 745–754; c) L. Baltzer, H. Nilsson, J. Nilsson, *Chem. Rev.* **2001**, *101*, 3153–3164; d) K. J. Jensen, in: *Peptide and Protein Design for Biopharmaceutical Applications* (Ed.: K. J. Jensen), John Wiley & Sons, Chichester, **2009**, pp. 207–248.

[7] a) A. R. Sanford, K. Yamato, X. Yang, L. Yuan, Y. Han, B. Gong, *Eur. J. Biochem.* **2004**, *271*, 1416–1425; b) J. L. Price, W. S. Horne, S. H. Gellman, *J. Am. Chem. Soc.* **2007**, *129*, 6376–6377; c) W. Cai, G.-T. Wang, P. Du, R.-X. Wang, X.-K. Jiang, Z.-T. Li, *J. Am. Chem. Soc.* **2008**, *130*, 13450–13459; d) A. Petitjean, L. A. Cuccia, M. Schmutz, J.-M. Lehn, *J. Org. Chem.* **2008**, *73*, 2481–2495; e) H. Goto, H. Katagiri, Y. Furusho, E. Yashima, *J. Am. Chem. Soc.* **2006**, *128*, 7176–7178; f) H. Goto, Y. Furusho, K. Miwa, E. Yashima, *J. Am. Chem. Soc.* **2009**, *131*, 4710–4719; g) V. Berl, M. J. Krische, I. Huc, J.-M. Lehn, M. Schmutz, *Chem. Eur. J.* **2000**, *6*, 1938–1946; h) C. Bao, Q. Gan, B. Kauffmann, H. Jiang, I. Huc, *Chem. Eur. J.* **2009**, *15*, 11530–11536; i) Y. Ferrand, A. M. Kendhale, J. Garric, B. Kauffmann, I. Huc, *Angew. Chem.* **2010**, *122*, 1822–1825; *Angew. Chem. Int. Ed.* **2010**, *49*, 1778–1781; j) N. Delsuc, S. Massip, J.-M. Léger, B. Kauffmann, I. Huc, *J. Am. Chem. Soc.* **2011**, *133*, 3165–3172; k) I. M. Mándity, L. Fülöp, E. Vass, G. K. Tóth, T. A. Martinek, F. Fülöp, *Org. Lett.* **2010**, *12*, 5584–5587.

[8] J. Becerril, J. M. Rodriguez, I. Saraogi, A. D. Hamilton, in: *Foldamers* (Eds.: S. Hecht, I. Huc), Wiley-VCH, Weinheim, Germany, **2007**, pp. 195–228.

[9] a) R. B. Prince, S. A. Barnes, J. S. Moore, *J. Am. Chem. Soc.* **2000**, *122*, 2758–2762; b) A. Tanatani, M. J. Mio, J. S. Moore, *J. Am. Chem. Soc.* **2001**, *123*, 1792–1793; c) A. Tanatani, T. S. Hughes, J. S. Moore, *Angew. Chem.* **2002**, *114*, 335–338; *Angew. Chem. Int. Ed.* **2002**, *41*, 325–328; d) M. T. Stone, J. S. Moore,

Org. Lett. **2004**, *6*, 469–472; e) R. A. Smaldone, J. S. Moore, *Chem. Eur. J.* **2008**, *14*, 2650–2657.

[10] a) C. Bao, B. Kauffmann, Q. Gan, K. Srinivas, H. Jiang, I. Huc, *Angew. Chem.* **2008**, *120*, 4221–4224; *Angew. Chem. Int. Ed.* **2008**, *47*, 4153–4156; b) E. Berni, J. Garric, C. Lamit, B. Kauffmann, J.-M. Léger, I. Huc, *Chem. Commun.* **2008**, 1968–1970; c) Y. Ferrand, A. M. Kendhale, B. Kauffmann, A. Grélard, C. Marie, V. Blot, M. Pipelier, D. Dubreuil, I. Huc, *J. Am. Chem. Soc.* **2010**, *132*, 7858–7859.

[11] a) M. Inouye, M. Waki, H. Abe, *J. Am. Chem. Soc.* **2004**, *126*, 2022–2027; b) H. Abe, N. Masuda, M. Waki, M. Inouye, *J. Am. Chem. Soc.* **2005**, *127*, 16189–16196; c) M. Waki, H. Abe, M. Inouye, *Angew. Chem.* **2007**, *119*, 3119–3121; *Angew. Chem. Int. Ed.* **2007**, *46*, 3059–3061.

[12] a) J.-L. Hou, X.-B. Shao, G.-J. Chen, Y.-X. Zhou, X.-K. Jiang, Z.-T. Li, *J. Am. Chem. Soc.* **2004**, *126*, 12386–12394; b) H.-P. Yi, X.-B. Shao, J.-L. Hou, C. Li, X.-K. Jiang, Z.-T. Li, *New J. Chem.* **2005**, *29*, 1213–1218; c) C. Li, S.-F. Ren, J.-L. Hou, H.-P. Yi, S.-Z. Zhu, X.-K. Jiang, Z.-T. Li, *Angew. Chem.* **2005**, *117*, 5871–5875; *Angew. Chem. Int. Ed.* **2005**, *44*, 5725–5729; d) J.-L. Hou, H.-P. Yi, X.-B. Shao, C. Li, Z.-Q. Wu, X.-K. Jiang, L.-Z. Wu, C.-H. Tung, Z.-T. Li, *Angew. Chem.* **2006**, *118*, 810–814; *Angew. Chem. Int. Ed.* **2006**, *45*, 796–800; e) C. Li, G.-T. Wang, H.-P. Yi, X.-K. Jiang, Z.-T. Li, R.-X. Wang, *Org. Lett.* **2007**, *9*, 1797–1800.

[13] a) H. Juwarker, K.-S. Jeong, *Chem. Soc. Rev.* **2010**, *39*, 3664–3674 and references cited therein; b) K.-J. Chang, B.-N. Kang, M.-H. Lee, K.-S. Jeong, *J. Am. Chem. Soc.* **2005**, *127*, 12214–12215; c) U.-I. Kim, J.-m. Suk, V. R. Naidu, K.-S. Jeong, *Chem. Eur. J.* **2008**, *14*, 11406–11414; d) V. R. Naidu, M. C. Kim, J.-m. Suk, H.-J. Kim, M. Lee, E. Sim, K.-S. Jeong, *Org. Lett.* **2008**, *10*, 5373–5376; e) H. Juwarker, J. M. Lenhardt, D. M. Pham, S. L. Craig, *Angew. Chem.* **2008**, *120*, 3800–3803; *Angew. Chem. Int. Ed.* **2008**, *47*, 3740–3743; f) R. M. Meudtner, S. Hecht, *Angew. Chem.* **2008**, *120*, 5004–5008; *Angew. Chem. Int. Ed.* **2008**, *47*, 4926–4930; g) H. Juwarker, J. M. Lenhardt, J. C. Castillo, E. Zhao, S. Krishnamurthy, R. M. Jamiolkowski, K.-H. Kim, S. L. Craig, *J. Org. Chem.* **2009**, *74*, 8924–8934; h) Y. Wang, F. Bie, H. Jiang, *Org. Lett.* **2010**, *12*, 3630–3633; i) Y. Hua, A. H. Flood, *J. Am. Chem. Soc.* **2010**, *132*, 12838–12840; j) Y. Wang, J. Xiang, H. Jiang, *Chem. Eur. J.* **2011**, *17*, 613–619.

[14] a) G. Maayan, M. D. Ward, K. Kirshenbaum, *Proc. Natl. Acad. Sci. USA* **2009**, *106*, 13679–13684; b) M. M. Müller, M. A. Windsor, W. C. Pomerantz, S. H. Gellman, D. Hilvert, *Angew. Chem.* **2009**, *121*, 940–943; *Angew. Chem. Int. Ed.* **2009**, *48*, 922–925.

[15] a) L. Brunsveld, R. B. Prince, E. W. Meijer, J. S. Moore, *Org. Lett.* **2000**, *2*, 1525–1528; b) R. B. Prince, L. Brunsveld, E. W. Meijer, J. S. Moore, *Angew. Chem.* **2000**, *112*, 234–230; *Angew. Chem. Int. Ed.* **2000**, *39*, 228–230; c) H. Goto, J. M. Heemstra, D. J. Hill, J. S. Moore, *Org. Lett.* **2004**, *6*, 889–892.

[16] a) C. Dolain, V. Maurizot, I. Huc, *Angew. Chem.* **2003**, *115*, 2844–2846; *Angew. Chem. Int. Ed.* **2003**, *42*, 2738–2740; b) C. Dolain, H. Jiang, J.-M. Léger, P. Guionneau, I. Huc, *J. Am. Chem. Soc.* **2005**, *127*, 12943–12951; c) E. R. Gillies, F. Deiss, C. Staedel, J.-M. Schmitter, I. Huc, *Angew. Chem.* **2007**, *119*, 4159–4162; *Angew. Chem. Int. Ed.* **2007**, *46*, 4081–4084.

[17] a) A. Khan, C. Kaiser, S. Hecht, *Angew. Chem.* **2006**, *118*, 1912–1915; *Angew. Chem. Int. Ed.* **2006**, *45*, 1878–1881; b) A. Khan, S. Hecht, *Chem. Eur. J.* **2006**, *12*, 4764–4774.

[18] a) Y. Geng, A. Trajkovska, D. Katsis, J. J. Ou, S. W. Culligan, S. H. Chen, *J. Am. Chem. Soc.* **2002**, *124*, 8337–8347; b) T. Ben, H. Goto, K. Miwa, H. Goto, K. Morino, Y. Furusho, E. Yashima, *Macromolecules* **2008**, *41*, 4506–4509; c) H.-Y. Hu, J.-F. Xiang, Y. Yang, C.-F. Chen, *Org. Lett.* **2008**, *10*, 1275–1278; d) H. Abe, D. Murayama, F. Kayamori, M. Inouye, *Macromolecules* **2008**, *41*, 6903–6909; e) E. D. King, P. Tao, T. T. Sanan, C. M. Hadad, J. R. Parquette, *Org. Lett.* **2008**, *10*, 1671–1674; f) P. Rivera-Fuentes, J. L. Alonso-Gómez, A. G. Petrovic, F. Santoro, N. Harada, N. Berova, F. Diederich, *Angew. Chem.* **2010**, *122*, 2296–2300; *Angew. Chem. Int. Ed.* **2010**, *49*, 2247–2250.

[19] a) D. J. Hill, J. S. Moore, *Proc. Natl. Acad. Sci. USA* **2002**, *99*, 5053–5057; b) H. Sugiura, Y. Nigorikawa, Y. Saiki, K. Nakamura, M. Yamaguchi, *J. Am. Chem. Soc.* **2004**, *126*, 14858–14864; c) P. K. Baruah, R. Gonnade, P. R. Rajamohanan, H.-J. Hofmann, G. J. Sanjayan, *J. Org. Chem.* **2007**, *72*, 5077–5084; d) H.-Y. Hu, J.-F. Xiang, Y. Yang, C.-F. Chen, *Org. Lett.* **2008**, *10*, 69–72; e) R. Amemiya, N. Saito, M. Yamaguchi, *J. Org. Chem.* **2008**, *73*, 7137–7144; f) M. Miyasaka, M. Pink, S. Rajca, A. Rajca, *Angew. Chem.* **2009**, *121*, 6068–6071; *Angew. Chem. Int. Ed.* **2009**, *48*, 5954–5957.

[20] X. Jiang, Y.-K. Lim, B. J. Zhang, E. A. Opsitnick, M.-H. Baik, D. Lee, *J. Am. Chem. Soc.* **2008**, *130*, 16812–16822.

[21] G. S. Kottas, L. I. Clarke, D. Horinek, J. Michl, *Chem. Rev.* **2005**, *105*, 1281–1376.

[22] W. R. Browne, D. Pijper, M. M. Pollard, B. L. Feringa, in: *From Non-Covalent Assemblies to Molecular Machines* (Eds.: J.-P. Sauvage, P. Gaspard), Wiley-VCH, Weinheim, Germany, **2011**, pp. 243–289.

[23] a) G. N. Lewis, T. T. Magel, D. Lipkin, *J. Am. Chem. Soc.* **1942**, *64*, 1774–1782; b) M. Sundaralingam, L. H. Jensen, *J. Am. Chem. Soc.* **1966**, *88*, 198–204.

[24] a) A. Ikeda, H. Udzu, Z. Zhong, S. Shinkai, S. Sakamoto, K. Yamaguchi, *J. Am. Chem. Soc.* **2001**, *123*, 3872–3877; b) S. Hiraoka, K. Harano, T. Tanaka, M. Shiro, M. Shionoya, *Angew. Chem.* **2003**, *115*, 5340–5343; *Angew. Chem. Int. Ed.* **2003**, *42*, 5182–5185; c) S. Hiraoka, K. Hirata, M. Shionoya, *Angew. Chem.* **2004**, *116*, 3902–3906; *Angew. Chem. Int. Ed.* **2004**, *43*, 3814–3818; d) S. Hiraoka, E. Okuno, T. Tanaka, M. Shiro, M. Shionoya, *J. Am. Chem. Soc.* **2008**, *130*, 9089–9098.

[25] a) J. A. Riddle, J. C. Bollinger, D. Lee, *Angew. Chem.* **2005**, *117*, 6847–6851; *Angew. Chem. Int. Ed.* **2005**, *44*, 6689–6693; b) J. A. Riddle, S. P. Lathrop, J. C. Bollinger, D. Lee, *J. Am. Chem. Soc.* **2006**, *128*, 10986–10987; c) X. Jiang, J. C. Bollinger, D. Lee, *J. Am. Chem. Soc.* **2006**, *128*, 11732–11733; d) J. A. Riddle, X. Jiang, J. Huffman, D. Lee, *Angew. Chem.* **2007**, *119*, 7149–7152; *Angew. Chem. Int. Ed.* **2007**, *46*, 7019–7022; e) Y.-K. Lim, S. Wallace, J. C. Bollinger, X. Chen, D. Lee, *Inorg. Chem.* **2007**, *46*, 1694–1703; f) Y.-K. Lim, X. Jiang, J. C. Bollinger, D. Lee, *J. Mater. Chem.* **2007**, *17*, 1969–1980; g) X. Jiang, M. C. Vieweger, J. C. Bollinger, B. Dragnea, D. Lee, *Org. Lett.* **2007**, *9*, 3579–3582; h) E. Opsitnick, D. Lee, *Chem. Eur. J.* **2007**, *13*, 7040–7049; i) M. Vieweger, X. Jiang, Y.-K. Lim, J. Jo, D. Lee, B. Dragnea, *J. Phys. Chem. A* **2011**, *115*, 13298–13308.

[26] a) J. H. Chong, M. Sauer, B. O. Patrick, M. J. MacLachlan, *Org. Lett.* **2003**, *5*, 3823–3826; b) M. Sauer, C. Yeung, J. H. Chong, B. O. Patrick, M. J. MacLachlan, *J. Org. Chem.* **2006**, *71*, 775–788.

[27] a) C. V. Yelamaggad, A. S. Achalkumar, D. S. S. Rao, S. K. Prasad, *J. Am. Chem. Soc.* **2004**, *126*, 6506–6507; b) C. V. Yelamaggad, A. S. Achalkumar, D. S. S. Rao, S. K. Prasad, *J. Org. Chem.* **2007**, *72*, 8308–8318; c) C. V. Yelamaggad, A. S. Achalkumar, D. S. S. Rao, S. K. Prasad, *J. Mater. Chem.* **2007**, *17*, 4521–4529; d) C. V. Yelamaggad, A. S. Achalkumar, D. S. S. Rao, S. K. Prasad, *J. Org. Chem.* **2009**, *74*, 3168–3171; e) C. V. Yelamaggad, R. Prabhu, D. S. S. Rao, S. K. Prasad, *Tetrahedron Lett.* **2010**, *51*, 4579–4583.

[28] a) N. Harada, K. Nakanishi, *Acc. Chem. Res.* **1972**, *5*, 257–263; b) N. Berova, K. Nakanishi, in: *Exciton Chirality Method: Principles and Applications* (Eds.: N. Berova, K. Nakanishi, R. W. Woody), Wiley-VCH, New York, **2000**, pp. 337–382; c) N. Berova, L. Di Bari, G. Pescitelli, *Chem. Soc. Rev.* **2007**, *36*, 914–931; d) N. Berova, B. Borhan, J. G. Dong, J. Guo, X. Huang, E. Karnaukhova, A. Kawamura, J. Lou, S. Matile, K. Nakanishi, B. Rickman, J. Su, Q. Tan, I. Zanze, *Pure Appl. Chem.* **1998**, *70*, 377–383; e) S. G. Allenmark, *Nat. Prod. Rep.* **2000**, *17*, 145–155.

[29] See the Supporting Information.

[30] a) J. A. Marshall, X. J. Wang, *J. Org. Chem.* **1992**, *57*, 1242–1252; b) W. R. Roush, R. J. Sciotti, *J. Am. Chem. Soc.* **1994**, *116*, 6457–6458; c) A. G. Myers, B. Zheng, *J. Am. Chem. Soc.* **1996**, *118*, 4492–4493; d) B. M. Trost, A. H. Weiss, *Adv. Synth. Catal.* **2009**, *351*, 963–983; e) P. J. Stang, F. Diederich, in: *Modern Acetylene Chemistry*, VCH, Weinheim, Germany, **1995**; f) F. Diederich, P. J. Stang, R. R. Tykwinski, in: *Acetylene Chemistry: Chemistry, Biology, and Material Science*, Wiley-VCH, Weinheim, Germany, **2005**.

[31] a) L. Pu, H.-B. Yu, *Chem. Rev.* **2001**, *101*, 757–824; b) L. Pu, *Tetrahedron* **2003**, *59*, 9873–9886; c) P. G. Cozzi, R. Hilgraf, N. Zimmermann, *Eur. J. Org. Chem.* **2004**, 4095–4105; d) D. E. Frantz, R. Fässler, C. S. Tomooka, E. M. Carreira, *Acc. Chem. Res.* **2000**, *33*, 373–381; e) P. Aschwanden, E. M. Carreira, in: *Acetylene Chemistry: Chemistry, Biology, and Material Science* (Eds.: F. Diederich, P. J. Stang, R. R. Tykwinski), Wiley-VCH, Weinheim, Germany, **2005**, pp. 101–138.

[32] a) H. C. Brown, P. V. Ramachandran, *Acc. Chem. Res.* **1992**, *25*, 16–24; b) C. J. Helal, P. A. Magriotis, E. J. Corey, *J. Am. Chem. Soc.* **1996**, *118*, 10938–10939; c) K. Matsumura, S. Hashiguchi, T. Ikariya, R. Noyori, *J. Am. Chem. Soc.* **1997**, *119*, 8738–8739; d) T. Ikariya, A. J. Blacker, *Acc. Chem. Res.* **2007**, *40*, 1300–1308.

[33] a) E. García-Urdiales, I. Alfonso, V. Gotor, *Chem. Rev.* **2005**, *105*, 313–354; b) P. Allevi, P. Ciuffreda, M. Anastasia, *Tetrahedron: Asymmetry* **1997**, *8*, 93–99; c) J.-L. Abad, C. Soldevila, F. Camps, P. Clapés, *J. Org. Chem.* **2003**, *68*, 5351–5356; d) D. Xu, Z. Li, S. Ma, *Tetrahedron Lett.* **2003**, *44*, 6343–6346; e) D. Xu, Z. Lu, Z. Li, S. Ma, *Tetrahedron* **2004**, *60*, 11879–11887; f) C. Raminelli, J. V. Comasseto, L. H. Andrade, A. L. M. Porto, *Tetrahedron: Asymmetry* **2004**, *15*, 3117–3122.

[34] a) D. E. Frantz, R. Fässler, E. M. Carreira, *J. Am. Chem. Soc.* **2000**, *122*, 1806–1807; b) N. K. Anand, E. M. Carreira, *J. Am. Chem. Soc.* **2001**, *123*, 9687–9688; c) D. Boyall, D. E. Frantz, E. M. Carreira, *Org. Lett.* **2002**, *4*, 2605–2606.

[35] a) J. S. Cha, D. Y. Lee, J. M. Kim, *Org. Prep. Proced. Int.* **1999**, *31*, 694–697; b) J. S. Cha, J. H. Park, D. Y. Lee, *Bull. Korean Chem. Soc.* **2001**, *22*, 325–326.

[36] On the chiral HPLC matrix used in Figure S2 in the Supporting Information, the *R* isomer of the commercially available 1-phenylprop-2-yn-1-ol (i.e., X = H in Scheme 3) also has a shorter retention time than the *S* isomer.

[37] T. R. Hoye, C. S. Jeffrey, F. Shao, *Nat. Protoc.* **2007**, *2*, 2451–2458 and references cited therein.

[38] a) E. Keinan, M. Peretz, *J. Org. Chem.* **1983**, *48*, 5302–5309; b) E. J. Corey, A. Tramontano, *J. Am. Chem. Soc.* **1984**, *106*, 462–463; c) T. Ishikawa, M. Okano, T. Aikawa, S. Saito, *J. Org. Chem.* **2001**, *66*, 4635–4642.

[39] M. Ishizaki, O. Hoshino, *Tetrahedron* **2000**, *56*, 8813–8819.

[40] J. G. Rodríguez, J. Esquivias, A. Lafuente, C. Díaz, *J. Org. Chem.* **2003**, *68*, 8120–8128.

[41] D. Neuhaus, M. P. Williamson, *The Nuclear Overhauser Effect in Structural and Conformational Analysis*, Wiley-VCH, New York, **2000**.

[42] Variable-temperature (VT) ^{1}H NMR studies on $(S,S)_3$-**4** in [D$_7$]toluene (T = 283–343 K) gave $\Delta H = 3.9 \pm 0.3$ kcal mol^{-1} and $\Delta S = 9.0 \pm 0.8$ cal mol^{-1} K^{-1} for the idealized two-state switching between the *folded* and *unfolded* conformer (Figure S4 in the Supporting Information). Under similar conditions, the reference system $(S,S)_3$-**2** has $\Delta H = 2.2 \pm 0.1$ kcal mol^{-1} and $\Delta S = 4.2 \pm 0.1$ cal mol^{-1} K^{-1}.[20] An increased enthalpic cost of disrupting the O–H···O hydrogen bonding network of $(S,S)_3$-**4** relative to that of $(S,S)_3$-**2** suggests an enhanced thermodynamic bias toward the "correctly" folded form of the molecule with bulkier π-substituents. This observation is consistent with the CD data shown in Figure 7, although care should be taken in comparing data obtained in different solvent systems.

[43] C. Reichardt, T. Welton, *Solvents and Solvent Effects in Organic Chemistry*, 4th ed., Wiley-VCH, Weinheim, Germany, **2010**.

[44] G. A. Hembury, V. V. Borovkov, Y. Inoue, *Chem. Rev.* **2008**, *108*, 1–73.

[45] a) X. Huang, B. H. Rickman, B. Borhan, N. Berova, K. Nakanishi, *J. Am. Chem. Soc.* **1998**, *120*, 6185–6186; b) T. Kurtán, N. Nesnas, Y.-Q. Li, X. Huang, K. Nakanishi, N. Berova, *J. Am. Chem. Soc.* **2001**, *123*, 5962–5973; c) X. Huang, N. Fujioka, G. Pescitelli, F. E. Koehn, R. T. Williamson, K. Nakanishi, N. Berova, *J. Am. Chem. Soc.* **2002**, *124*, 10320–10335; d) J. M. Lintuluoto, V. V. Borovkov, Y. Inoue, *J. Am. Chem. Soc.* **2002**, *124*, 13676–13677; e) G. Proni, G. Pescitelli, X. Huang, K. Nakanishi, N. Berova, *J. Am. Chem. Soc.* **2003**, *125*, 12914–12927; f) X. Li, M. Tanasova, C. Vasileiou, B. Borhan, *J. Am. Chem. Soc.* **2008**, *130*, 1885–1893; g) X. Li, B. Borhan, *J. Am. Chem. Soc.* **2008**, *130*, 16126–16127.

[46] a) N. Ruangsupapichat, M. M. Pollard, S. R. Harutyunyan, B. L. Feringa, *Nat. Chem.* **2011**, *3*, 53–60, and references cited thereinb) J. Wang, B. L. Feringa, *Science* **2011**, *331*, 1429–1432; c) B. L. Feringa, R. A. van Delden, M. K. J. ter Wiel, in: *Chiroptical Molecular Switches* (Ed.: B. L. Feringa), Wiley-VCH, Weinheim, Germany, **2001**, pp. 123–163.

[47] PhotochemCAD, http://www.photochemcad.com.

[48] J. B. Armitage, N. Entwistle, E. R. H. Jones, M. C. Whiting, *J. Chem. Soc.* **1954**, 147–154.

[49] A. B. Pangborn, M. A. Giardello, R. H. Grubbs, R. K. Rosen, F. J. Timmers, *Organometallics* **1996**, *15*, 1518–1520.

[50] J. Iskra, S. Stavber, M. Zupan, *Synthesis* **2004**, 1869–1873.

[51] K.-J. Chang, D. Moon, M. S. Lah, K.-S. Jeong, *Angew. Chem.* **2005**, *117*, 8140–8143; *Angew. Chem. Int. Ed.* **2005**, *44*, 7926–7929.

Received: September 15, 2011
Published Online: December 2, 2011

